A Robust Generalized Modified Blake–Zisserman Adaptive Filter-Based Control Scheme for Grid-Tied PV System to Improve Power Quality

Markala Karthik
Department of Electrical Engineering
National Institute of Technology Rourkela
Odisha, India
markalakarthikreddy@gmail.com

Venkata Ramana Naik N
Department of Electrical Engineering
National Institute of Technology Rourkela
Odisha, India
nenavathv@nitrkl.ac.in

Anup Kumar Panda
Department of Electrical Engineering
National Institute of Technology Rourkela
Odisha, India
akpanda@nitrkl.ac.in

***Abstract*— This paper presents a robust generalized modified Blake–Zisserman adaptive filter (GMBZAF)-based control scheme for a three-phase grid-tied single-stage photovoltaic system (GTPVS) to improve power quality (PQ). The GMBZAF-based control scheme enables GTPVS to integrate maximum PV power into the grid with power quality (PQ) improvement at the grid side, such as maintaining balanced sinusoidal grid currents, current harmonics mitigation, reactive power assistance to the inductive load at steady-state, and even during dynamic conditions (variable load and irradiance). The GMBZAF is implemented to accurately calculate the active and reactive weight components of load current. The GTPVS is modeled using MATLAB/Simulink, and its response is observed at steady-state, unbalanced loading, and variable solar irradiance conditions. The comparative assessment between the proposed control scheme and the existing adaptive filtering-based control schemes such as least mean square (LMS) and least mean fourth (LMF) is done.**

Keywords*— *Blake-Zisserman Adaptive Filter, Least Mean Fourth, Least Mean Square, Photovoltaic, Power Quality.

I. INTRODUCTION

Renewable energy sources have gained significant interest in global electrical energy generation due to exponentially rising energy consumption and environmental challenges caused by fossil fuels. Solar energy is becoming popular due to decreasing cost of photovoltaic (PV) modules, less maintenance, and clean energy, which is easily captured. Generally, two types of topologies are available in the literature for the grid-tied PV system (GTPVS): single-stage and double-stage, each having merits and demerits [1]. When the power loss, efficiency, system complexity, and reliability are considered, a single-stage topology is preferred. When the PV array's output voltage is insufficient for the DC link to have power flow, it is preferable to use a double-stage topology where a dc-dc converter is employed additionally. The double-stage topology shares the control burden among dc-dc converter and VSC. An effective control scheme is the heart of the operation for GTPVS. The control scheme operates GTPVS such that it enables GTPVS to provide multi functionalities such as integrating the maximum PV power into the grid with grid side power quality (PQ) improvement, thus maintaining balanced sinusoidal grid currents, current harmonics mitigation, and reactive power assistance to inductive load while feeding nonlinear loads. To calculate the fundamental component from the distorted signal, several traditional techniques based on transformations and phase-locked loop (PLL) [2] have been reported in the literature. In the PLL-based synchronous reference frame (SRF), the low pass filter contributed to oscillations, which reduced the system's ability to respond dynamically. This issue prevailed in the direct axis component of current. Control schemes based on adaptive filtering algorithms such as variable step-size LMS [3], least mean fourth [4], and least logarithmic absolute difference (LLAD) [5] are utilized to calculate fundamental weight component of distorted current. The filtering schemes' accuracy, steady state alignment, and dynamic response depend on non-gaussian environmental conditions. It is essential to embed an appropriate cost function to derive the weights updating relation specifically for various noise environments. Several adaptive filtering-based control schemes are embedded with different cost functions like different powers of the error, mean absolute third error [6], and sigmoid [7]. The accuracy of adaptive filters is improved by including the robust generalized modified Blake–Zisserman(GMBZAF) [8] cost function in updating the weights thus leading to a GMBZAF-based control scheme. The convergence performance of GMBZAF is superior to that of other existing algorithms.

The major contributions of this paper are:

- Injection of maximum power from PV array into grid along with the improvement of PQ at grid side.
- Calculation of fundamental weight components of distorted nonlinear load current using GMBZAF.
- Maintaining grid currents sinusoidal at unity power factor (UPF) while feeding nonlinear loads.

This paper is organized into five sections. Section II presents GTPVS configuration. Section III presents the overall control scheme for single-stage GTPVS based on the proposed GMBZAF-based control scheme. Section IV contains the results and discussion. The conclusion of this paper is presented in Section V.

II. GTPVS CONFIGURATION

The single-stage GTPVS configuration is shown in Fig. 1. It is formed by an IGBT-based voltage source converter (VSC), PV array, dc-link capacitance (C_{dc}), ripple filter (R_{rf} and C_{rf}), and interfacing inductance (L_f). The GTPVS parameters are designed as illustrated in [3].

III. PROPOSED GMBZAF-BASED CONTROL SCHEME FOR GTPVS

The GMBZ cost function is [8]

$$J(e(r)) = \log(1+\delta) - E\left\{\log\left[\exp\left(-\rho\left|e(r)\right|^{\beta}\right)\right] + \delta\right\} \quad (1)$$

where e(r) is an adaptive error component, δ is a normalization constant, β is a shape parameter, ρ is a parameter controlling kernel width, and E[.] is the expectation operator. Here δ, β and ρ are the non-zero positive parameters. The GMBZ cost function exhibits a more robust behavior in reducing the adaptive error and improving convergence than

978-1-6654-5566-4/22/$31.00 ©2022 IEEE

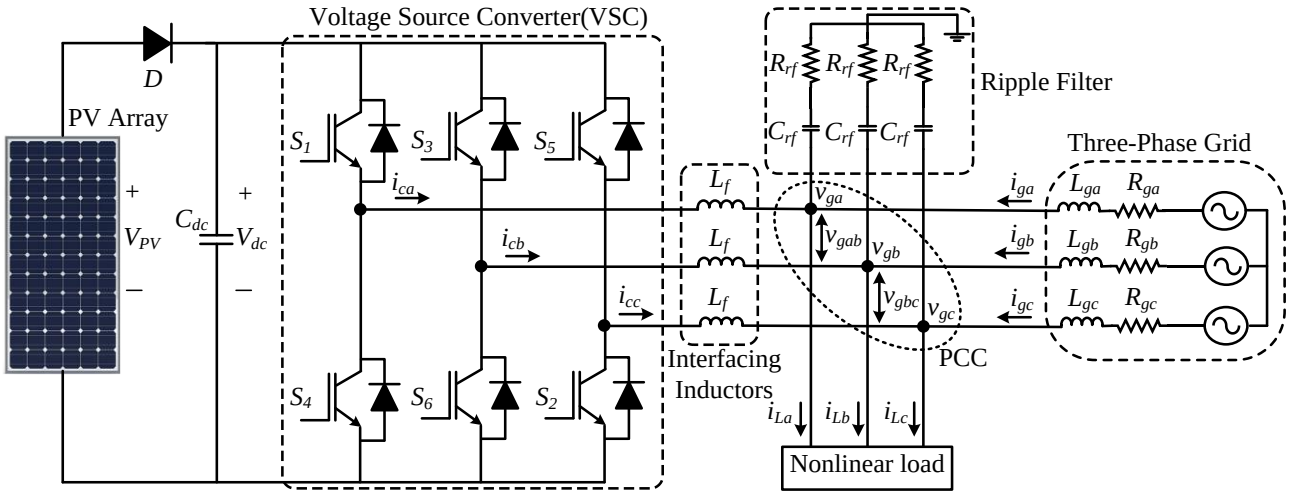

Fig. 1. GTPVS configuration

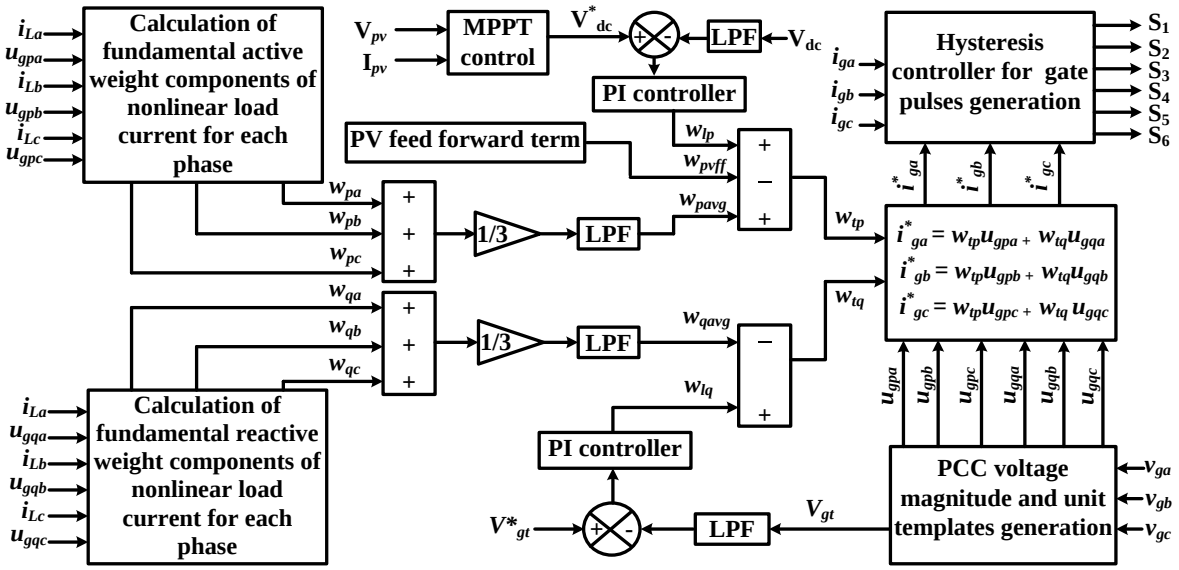

Fig. 2. Control architecture for GTPVS

most existing cost functions. It reduces steady-state misalignment. The GMBZAF weights are updated with a step size of 'μ' using (2)

$$w(r+1) = w(r) + \mu f(e(r))u(r) \tag{2}$$

where,

$$f(e(r)) = \frac{\exp\left(-\rho|e(r)|^{\beta}\right)|e(r)|^{\beta-1} sign[e(r)]}{\left[\delta + \exp\left(-\rho|e(r)|^{\alpha}\right)\right]} \tag{3}$$

The control architecture for single-stage GTPVS is shown in Fig. 2 and is divided into four sections as explained below.

A. *Extraction of Maximum Power from PV Array*

An incremental conductance (InC) -based MPPT [9] is used for PV array to deliver maximum power in which the operating point is updated to reach maximum power point (MPP). The PV voltage at MPP is considered as the reference dc-link voltage in implementing a control scheme. The equations and P_{PV}-V_{PV} characteristics of PV array illustrating the operation of InC MPPT method are given as (4)-(7) and in Fig. 3.

$$\frac{dP_{PV}}{dV_{PV}} = I_{PV} + V_{PV}\frac{dI_{PV}}{dV_{PV}} = G + \Delta G = 0 \tag{4}$$

$$\Delta G > -G, \text{ left to MPP} \tag{5}$$

$$\Delta G < -G, \text{ right to MPP} \tag{6}$$

$$\Delta G = -G, \text{ at MPP} \tag{7}$$

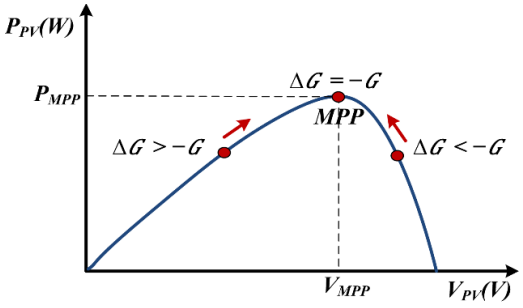

Fig. 3. P_{PV}-V_{PV} characteristics of PV array illustrating InC MPPT method

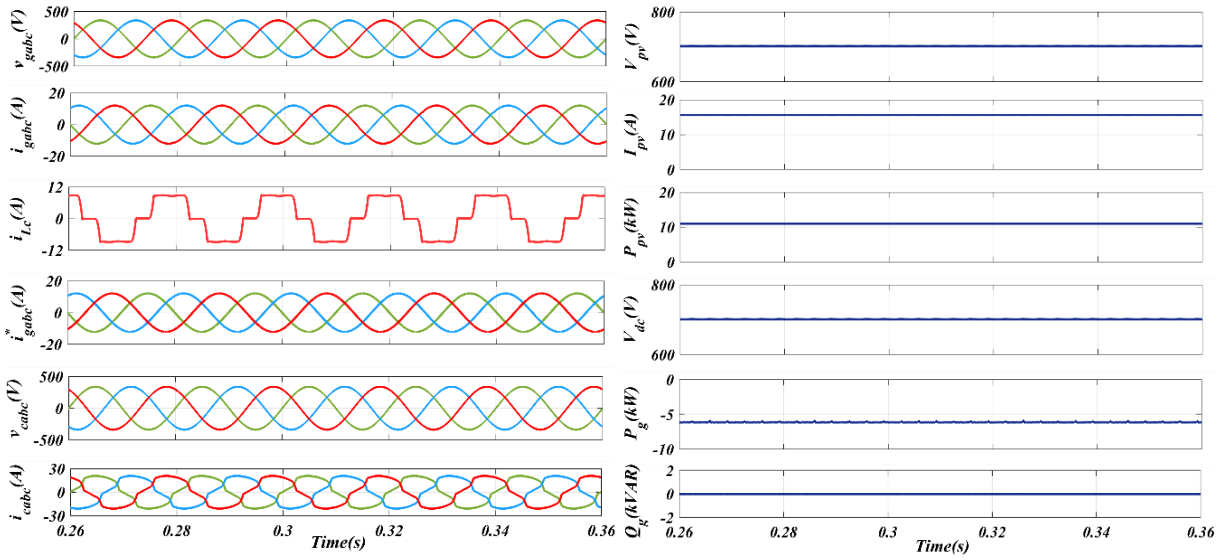

(a) (b)

Fig. 4 (a) and (b): Performance of GTPVS during steady-state operating condition with balanced nonlinear load

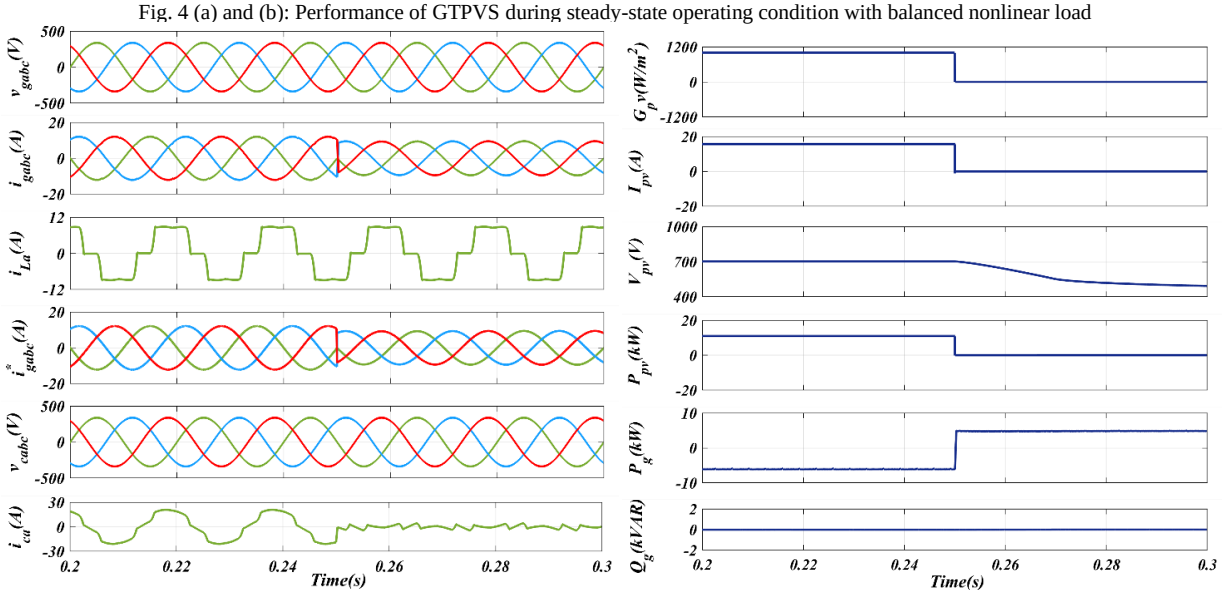

(a) (b)

Fig. 5 (a) and (b): Dynamic performance of GTPVS during a change in irradiation

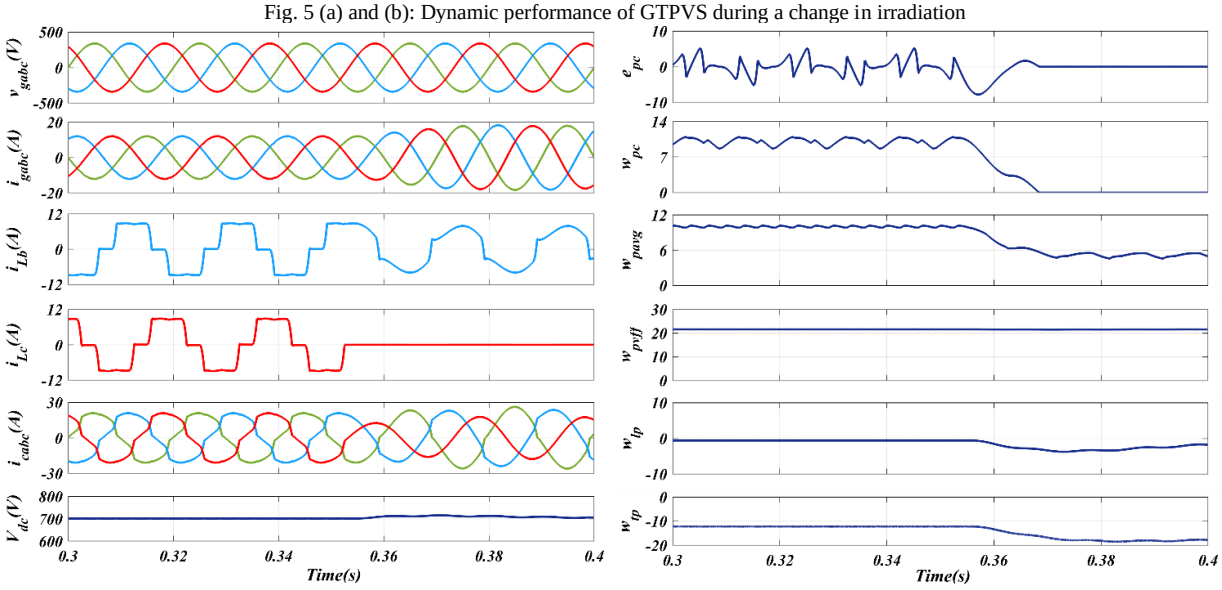

(a) (b)

Fig. 6 (a) and (b): Dynamic performance of GTPVS during unbalanced load

B. Generation of PCC Unit Voltage Templates

The point of common coupling (PCC) phase voltages are calculated from the sensed PCC line voltages, and then PCC voltage maximum value is calculated as [10]

$$\begin{bmatrix} v_{ga} \\ v_{gb} \\ v_{gc} \end{bmatrix} = \frac{1}{3}\begin{bmatrix} 2 & 1 \\ -1 & 1 \\ -1 & -2 \end{bmatrix}\begin{bmatrix} v_{gab} \\ v_{gbc} \end{bmatrix} \tag{8}$$

$$V_{gt} = \sqrt{2(v_{ga}^2 + v_{gb}^2 + v_{gc}^2)/3} \tag{9}$$

The in-phase unit and quadrature unit templates of PCC phase voltages are calculated as [11]

$$\begin{bmatrix} u_{gpa} \\ u_{gpb} \\ u_{gpc} \end{bmatrix} = \begin{bmatrix} v_{ga} \\ v_{gb} \\ v_{gc} \end{bmatrix}\begin{bmatrix} \frac{1}{V_{gt}} & \frac{1}{V_{gt}} & \frac{1}{V_{gt}} \end{bmatrix} \tag{10}$$

$$\begin{bmatrix} u_{gqa} \\ u_{gqb} \\ u_{gqc} \end{bmatrix} = \frac{1}{2\sqrt{3}}\begin{bmatrix} 0 & -2 & 2 \\ 3 & 1 & -1 \\ -3 & 1 & -1 \end{bmatrix}\begin{bmatrix} u_{gpa} \\ u_{gpb} \\ u_{gpc} \end{bmatrix} \tag{11}$$

C. Calculation of Weight Components

To inject the sinusoidal currents into grid, the weight of the fundamental active and reactive components of three phases *(a, b, c)* load currents are calculated using GMBZAF weights updating relation (12) and (13)

$$\begin{bmatrix} w_{pa}(r+1) \\ w_{pb}(r+1) \\ w_{pc}(r+1) \end{bmatrix} = \begin{bmatrix} w_{pa}(r) + \mu f(e_{pa}(r))u_{gpa}(r) \\ w_{pb}(r) + \mu f(e_{pb}(r))u_{gpb}(r) \\ w_{pc}(r) + \mu f(e_{pc}(r))u_{gpc}(r) \end{bmatrix} \tag{12}$$

$$\begin{bmatrix} w_{qa}(r+1) \\ w_{qb}(r+1) \\ w_{qc}(r+1) \end{bmatrix} = \begin{bmatrix} w_{qa}(r) + \mu f(e_{qa}(r))u_{gqa}(r) \\ w_{qb}(r) + \mu f(e_{qb}(r))u_{gqb}(r) \\ w_{qc}(r) + \mu f(e_{qc}(r))u_{gqc}(r) \end{bmatrix} \tag{13}$$

where, the adaptive error active and reactive components for three-phase load currents are given as

$$\begin{bmatrix} e_{pa}(r) \\ e_{pb}(r) \\ e_{pc}(r) \end{bmatrix} = \begin{bmatrix} i_{La}(r) - u_{gpa}(r)w_{pa}(r) \\ i_{Lb}(r) - u_{gpb}(r)w_{pb}(r) \\ i_{Lc}(r) - u_{gpc}(r)w_{pc}(r) \end{bmatrix} \tag{14}$$

$$\begin{bmatrix} e_{qa}(r) \\ e_{qb}(r) \\ e_{qc}(r) \end{bmatrix} = \begin{bmatrix} i_{La}(r) - u_{gqa}(r)w_{qa}(r) \\ i_{Lb}(r) - u_{gqb}(r)w_{qb}(r) \\ i_{Lc}(r) - u_{gqc}(r)w_{qc}(r) \end{bmatrix} \tag{15}$$

Consideration of the average for weight components is useful for maintaining balance among grid currents.

$$w_{pavg} = (w_{pa} + w_{pb} + w_{pc})/3 \tag{16}$$

$$w_{qavg} = (w_{qa} + w_{qb} + w_{qc})/3 \tag{17}$$

The response of grid currents is improved during dynamic variation of irradiance by involving the PV feedforward component (w_{pvff}) in the control scheme.

$$w_{pvff} = 2V_{pv}I_{pv}/3V^*_{gt} \tag{18}$$

A proportional-integral (PI) controller action on dc-link error voltage and PCC voltage error is employed to calculate active and reactive loss components *($w_{lp}(r+1)$, $w_{lq}(r+1)$)* to include in a control scheme.

$$w_{lp}(r+1) = w_{lp}(r) + K_{pdc}(V_{dce}(r+1) - V_{dce}(r)) + K_{idc}V_{dce}(r+1)) \tag{19}$$

$$w_{lq}(r+1) = w_{lq}(r) + K_{pac}(V_{gte}(r+1) - V_{gte}(r)) + K_{iac}V_{gte}(r+1)) \tag{20}$$

where, $V_{dce}(r) = V^*_{dc}(r) - V_{dc}(r)$ (21)

$$V_{gte}(r) = V^*_{gt}(r) - V_{gt}(r) \tag{22}$$

K_{pdc} and K_{idc} are dc-link PI controller parameters**,** K_{pac} and K_{iac} are PCC voltage PI controller parameters.

D. Calculation Grid Reference Sinusoidal Currents

The grid reference sinusoidal currents are calculated using the above-calculated weight components and unit templates as

$$i^*_{ga} = w_{tp}u_{gpa} + w_{tq}u_{gqa} \tag{23}$$

$$i^*_{gb} = w_{tp}u_{gpb} + w_{tq}u_{gqb} \tag{24}$$

$$i^*_{gc} = w_{tp}u_{gpc} + w_{tq}u_{gqc} \tag{25}$$

where, w_{tp} and w_{tq} are the total weight active and reactive components.

$$w_{tp} = w_{pavg} + w_{lp} - w_{pvff} \tag{26}$$

$$w_{tq} = w_{lq} - w_{qavg} \tag{27}$$

The calculated grid reference currents and sensed grid currents are passed through a hysteresis controller of width 0.01 to generate the driving pulses for VSC switches.

IV. Results And Discussion

The GTPVS is developed using MATLAB/Simulink. The number of PV array modules chosen to obtain a power of 11kW. A nonlinear load of 5kW is realized using a diode bridge rectifier and a series R-L load.

A. Performance of GTPVS During Steady-state Operating Condition with Balanced Nonlinear Load

Fig.4 (a) and (b) depicts the performance of GTPVS during steady-state operating condition with a balanced nonlinear load where the grid currents are maintained sinusoidal at unity power factor (UPF) with 6kW of PV power integrated to gird after supplying to 5kW nonlinear load. The grid currents are 180^o out of phase with grid voltages and grid reactive power *(Q_g)* is zero indicating no reactive power burden on grid. The dc-link voltage follows its reference voltage.

B. Performance of GTPVS During Dynamic Operating Conditions

The performance of GTPVS during dynamic condition is presented for two cases with a change in irradiation in Fig.5 (a) and (b) and unbalanced load depicted in Fig.6 (a) and (b).

1) Change in Irradiation from 1000 W/m^2 to Zero: When irradiation is decreased to zero from 1000 W/m^2 at 0.25 s, the power injecting to grid is changed from -6kW to 5kW indicating power is delivered to grid from PV after fulfilling load till 0.25 s. After 0.25 s the load power is supplied by grid

alone as there is no PV power. Now the VSC continues its functioning as a distribution static compensator (DSTATCOM) to solve PQ problems (load currents harmonics mitigation and reactive power compensation). The grid currents are in phase with the grid phase voltages here, indicating that the grid is delivering power to the load at UPF.

2) Unbalanced Nonlinear Load: Unbalanced load is realized by removing the phase '*c*' of the load at 0.35 s. The grid currents are balanced and sinusoidal, but their magnitude is increased due to simultaneous reduction of load power and injection of PV power. Magnitude of VSC currents(i_{cabc}) is changed to unbalanced to make the grid currents balanced. The adaptive error of phase '*c*' is reached to zero and weight components (w_{pc}, w_{pavg}, w_{lp}, w_{tp}) settle to new stable values immediately after unbalance is created in the load.

C. *Comparative Assessment of Proposed Control Scheme with Existing Control Schemes*

Fig. 7 depicts the average fundamental active weight component (w_{pavg}) calculated by the proposed control scheme, LMS, and LMF and Table I shows the comparative assessment among these control schemes when phase '*c*' of the load is removed from 0.35 s to 0.45 s to create an unbalance in the load. The proposed GMBZAF-based control scheme exhibits smooth variations and almost zero oscillations during steady state and less magnitude oscillations during dynamic conditions compared to that of LMS and LMF-based control schemes.

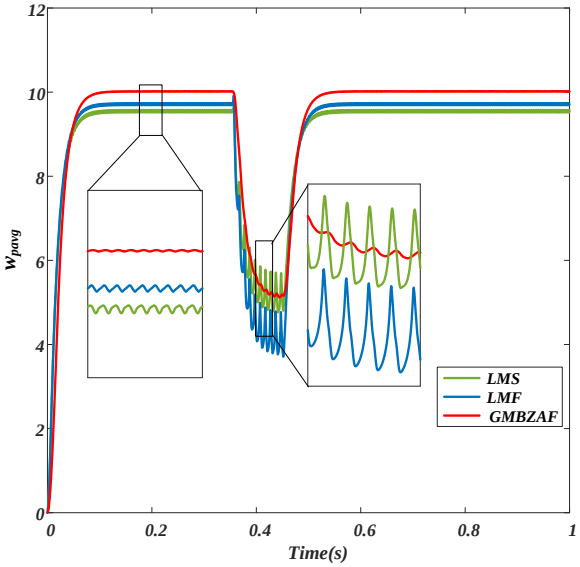

Fig. 7. Estimation of 'w_{pavg}' for proposed GMBZAF, LMS, and LMF-based control schemes

TABLE I. COMPARATIVE ASSESSMENT OF PROPOSED CONTROL SCHEMES WITH EXISTING CONTROL SCHEMES

Control Scheme	Steady state condition		Dynamic condition		
	Oscillations	*Accuracy*	*Oscillations*	*Tracking*	*Deviation*
LMS	High	Poor	More	Moderate	High
LMF	High	Poor	More	Fast	High
Proposed GMBZAF	less	Better	less	Fast	Less

D. *Total Harmonic Distortion (THD) calculation*

The THD of grid currents depicted in Fig. 8 (a) is 1.08%, held below the limit of IEEE-519 standard [12] while the nonlinear load current is having a THD of 25.51 % shown in Fig. 8 (b).

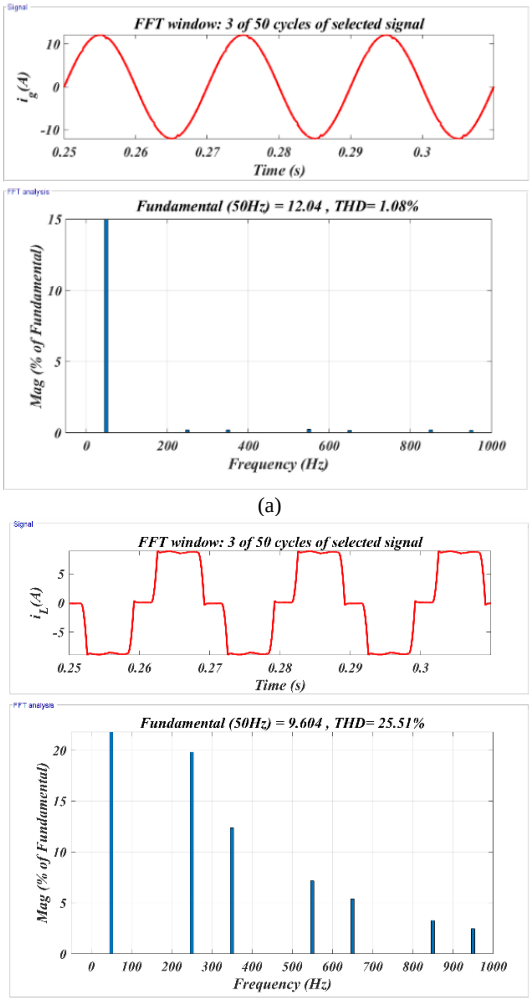

Fig. 8 (a) THD of grid current, and (b) THD of nonlinear load current

V. CONCLUSION

A robust GMBZAF-based control scheme is proposed for GTPVS, which mitigates the harmonics, providing a reactive power compensation, unbalanced load compensation, and maintaining grid currents sinusoidal at UPF, thus enhancing PQ while integrating PV power to grid. The performance of proposed GMBZAF-based control scheme is observed when GTPVS is operated in steady-state and dynamic operating conditions (variable load and irradiance) and it is observed that GMBZAF-based control scheme exhibits superior performance in terms of accuracy, convergence, and oscillations compared to LMS and LMF-based control schemes.

REFERENCES

[1] T. F. Wu, C. H. Chang, L. C. Lin, and C. L. Kuo, "Power loss comparison of single- and two-stage grid-connected photovoltaic systems," *IEEE Trans. Energy Convers.*, vol. 26, no. 2, pp. 707–715, Apr. 2011.

[2] K. Sridharan and B. Chitti Babu, "Accurate Phase Detection System Using Modified SGDFT-Based PLL for Three-Phase Grid-Interactive Power Converter During Interharmonic Conditions," *IEEE Trans. Instrum. Meas.*, vol. 71, p. 2022,Dec. 2021.

[3] Pradhan S, Hussain I, Singh B, and Panigrahi BK, "Modified VSS-LMS-based adaptive control for improving the performance of a single-stage PV-integrated grid system," *IET Sci. Meas. Technol.*, vol. 11, no. 4, pp. 388–399, Jul. 2017.

[4] R. K. Agarwal, I. Hussain, and B. Singh, "LMF-based control algorithm for single stage three-phase grid integrated solar PV system," *IEEE Trans. Sustain. Energy*, vol. 7, no. 4, pp. 1379–1387, Oct. 2016.

[5] N. Kumar, B. Singh, B. K. Panigrahi, and L. Xu, "Leaky-Least-Logarithmic-Absolute-Difference- InC MPPT Technique for Grid-Integrated PV system," *IEEE Trans. Ind. Electron.*, vol. 66, no. 11, pp. 9003–9012, Jan. 2019.

[6] H. Zhao, Y. Yu, S. Gao, X. Zeng, and Z. He, "A new normalized LMAT algorithm and its performance analysis," *Signal Processing*, vol. 105, pp. 399–409, Dec. 2014.

[7] F. Huang, J. Zhang, and S. Zhang, "A family of robust adaptive filtering algorithms based on sigmoid cost," *Signal Processing*, vol. 149, pp. 179–192, Aug. 2018.

[8] K. Kumar, M. L. N. S. Karthik, and N. V George, "Generalized Modified Blake – Zisserman Robust Sparse Adaptive Filters," *IEEE Trans. Syst., Man, Cybern., Syst.*, pp. 1–6, Jun. 2022.

[9] M. A. Abo-Sennah, M. A. El-Dabah, and A. E. B. Mansour, "Maximum power point tracking techniques for photovoltaic systems: A comparative study," *Int. J. Electr. Comput. Eng.*, vol. 11, no. 1, pp. 57–73, Feb. 2021.

[10] B. Singh, A. Chandra, and K. Al-Haddad, Power Quality Problems and Mitigating Techniques. London, U.K.: Wiley, 2015.

[11] P. Shukl and B. Singh, "Grid integration of three-phase single-stage PV system using adaptive Laguerre filter based control algorithm under nonideal distribution system," *IEEE Trans. Ind. Appl.*, vol. 55, no. 6, pp. 6193–6202, Dec. 2019.

[12] IEEE Recommended Practice and Requirements for Harmonic Control in Electric Power Systems, IEEE Std 519-2014, 2014.